Photoinduced Multiple Spectral Changes of Single Plasmonic Gold Nanospheres by the Aid of Coordination

Ichiro Tanabe and Tetsu Tatsuma*
Institute of Industrial Science, The University of Tokyo, 4-6-1 Komaba, Meguro-ku, Tokyo 153-8505

(E-mail: tatsuma@iis.u-tokyo.ac.jp)

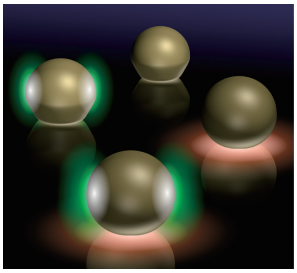

One or both of two localized surface plasmon modes (full-surface mode and interface mode) of a commercially available single Au nanosphere on TiO_2 are excited, and the corresponding spectral changes are induced in the presence of thiocyanate. Similar spectral changes can be simulated by assuming site-selective oxidation of the Au nanosphere by plasmon-induced charge separation (PICS).

REPRINTED FROM

Chemistry Letters

Vol.43 No.6 2014 p.931–933

CMLTAG
June 5, 2014

The Chemical Society of Japan

Received: February 25, 2014 | Accepted: March 20, 2014 | Web Released: March 28, 2014 CL-140153

Photoinduced Multiple Spectral Changes of Single Plasmonic Gold Nanospheres by the Aid of Coordination

Ichiro Tanabe† and Tetsu Tatsuma*
Institute of Industrial Science, The University of Tokyo, 4-6-1 Komaba, Meguro-ku, Tokyo 153-8505

(E-mail: tatsuma@iis.u-tokyo.ac.jp)

One or both of two localized surface plasmon modes (full-surface mode and interface mode) of a commercially available single Au nanosphere on TiO_2 are excited, and the corresponding spectral changes are induced in the presence of thiocyanate. Similar spectral changes can be simulated by assuming site-selective oxidation of the Au nanosphere by plasmon-induced charge separation (PICS).

Noble metal nanoparticles (NPs) exhibit strong absorption and scattering of light and generation of optical near field at specific wavelengths because of localized surface plasmon resonance (LSPR).[1–3] The LSPR wavelength depends largely on the particle size,[4,5] shape,[4,6] and dielectric environment.[7,8] By manipulating these factors, the LSPR wavelength can be controlled. Therefore, plasmonic metal NPs can be used for optical storage of images or data.[9,10] For multiple data storage, an ensemble of different NPs have been used.[9–12] We recently reported storage of 2-bit data in a single Ag NP, which is smaller than visible light wavelength, on the basis of selective excitation of one or both of the two LSPR modes (full-surface mode and interface mode).[13]

The data storage in single Ag NPs is based on plasmon-induced charge separation (PICS)[14,15] at a plasmonic NP–semiconductor interface. PICS is caused by electron transfer from plasmonic Au,[14,16] Ag,[9,16] and Cu[17] NPs to semiconductor, possibly due to an external photoelectric effect or hot electron injection. This phenomenon is applied to a wide range of fields, in particular photovoltaic cells and photosensors[14,18–21] as well as photocatalysis.[14,22] In the case of Ag NPs, their size and shape can be controlled by PICS under weak light,[11–13] because Ag is oxidized to Ag^+ preferentially at the sites where the plasmonic near field is strongly localized.[23] An ensemble of Ag NPs with different sizes on the TiO_2 semiconductor shows a broad absorption band over the visible region. If the ensemble is irradiated at a certain wavelength, only Ag NPs resonant at the wavelength are oxidized due to PICS, resulting in a wavelength-selective decrease of optical absorption. It allows multicolor photochromism and multiwavelength data storage.[9,11] By using a Ag nanorod ensemble with different aspect ratios, spectral dips can also form in the near-infrared region, leading to near-infrared photochromism.[12] The data storage in single Ag NPs is based on the site-selective oxidation of Ag NPs by excitation at two different wavelengths.[13]

However, the stored data are volatile, because Ag NPs on TiO_2 are gradually oxidized under ambient light unless the NPs are protected, for instance, with alkanethiol self-assembled monolayer (SAM).[24] This issue can be addressed by using Au, which is more stable than Ag because of more positive redox potential. However, Au NPs are not oxidized by PICS because of their high stability. In this study, we shift the redox potential of Au negatively[25] with the aid of coordination[26] and demonstrate PICS-based two-wavelength optical data storage in a commercially available single Au nanosphere. The recorded information is stable after the removal or inactivation of the ligands.[25]

A TiO_2 film was prepared on a Pyrex glass sheet from a ethanolic titanium alkoxide solution (NDH-510C, Nippon Soda) by a standard dip-coating technique (withdrawal rate was $2\,mm\,s^{-1}$, calcined at 500 °C for 1 h). Its thickness was ca. 150 nm and the surface roughness was ca. 10 nm. Commercially available monodisperse Au nanospheres (diameter: 150 nm, Tanaka Kikinzoku Kogyo) or Ag nanospheres (diameter: 100 nm, Sigma-Aldrich) were cast on the TiO_2 film ($50\,\mu L\,cm^{-2}$) and left in dark for 3 h or 5 min, respectively, followed by rinsing with ultrapure water. The optical properties of the single metal nanospheres were measured by dark-field microspectroscopy, in which scattering light from a plasmon-resonant NP can be observed.[3,13] Figure 1 shows typical dark-field images (obtained using BX-51, Olympus), corresponding scattering spectra (using C10027, Hamamatsu Photonics), and atomic force microscope (AFM) images (by NanoNavi Station/SPA400, SII Nanotechnology with Morphology Filter for elimination of the effect of the tip shape) of single Au (Figure 1a) and Ag (Figure 1b) nanospheres on TiO_2. The particle morphology can be precisely measured by AFM,[2,11] whereas a scattering light spot observed by dark-field microscopy is inevitably larger than the particle size[3,13] because of the diffraction limit and secondary scattering.

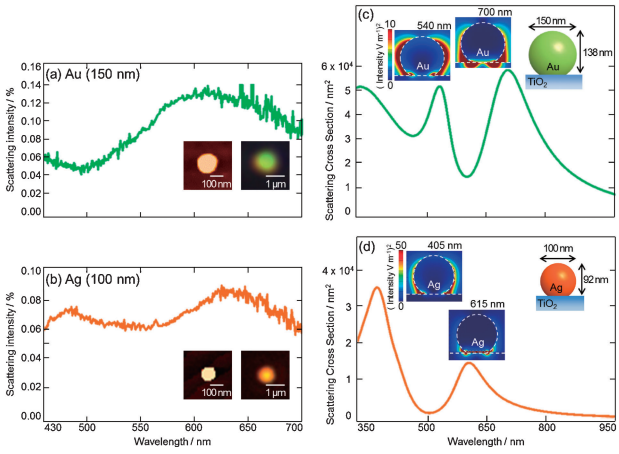

Figure 1. (a, b) Typical dark-field image, corresponding scattering spectra, and AFM images of a single (a) Au and (b) Ag nanosphere on TiO_2. (c, d) Scattering spectra and distributions of electric field intensity calculated by a FDTD method for a (c) Au and (d) Ag NP on TiO_2.

Au nanospheres exhibit a broad LSPR band from 500 to >700 nm and green scattering light. On the other hand, the Ag nanospheres show two LSPR bands in the shorter- and longer-wavelength regions than ca. 540 nm and orange scattering light. We have assigned the two bands of the Ag nanospheres to electric field oscillation distributed over the entire particle (full-surface mode) and that localized at around the Ag–TiO_2 interface (interface mode) by a finite-difference time-domain (FDTD) simulation on the basis of a model with a 100-nm Ag sphere whose bottom is cut by 8% on a flat TiO_2 (Figure 1d, inset; this model was optimized by spectral fitting).[13] In addition, we selectively excited one or both of the two modes, resulting in the selective suppression of the corresponding mode(s) and multiwavelength spectral changes.[13] In the case of the Au nanospheres, which exhibit only one broad LSPR band, multiple spectral control is not possible if the band is based on a single LSPR mode. However, if the band consists of more than one LSPR mode, the multiple control could be possible.

We, therefore, applied essentially the same model to the Au nanosphere. To examine the possibility that the single Au nanosphere has more than one LSPR mode, the scattering spectrum and electric field distribution were simulated based on the model with a 150-nm Au nanosphere whose bottom is cut by 8% (Figure 1c, inset). As shown in Figure 1c, the calculated scattering spectrum has two LSPR peaks at about 540 and 700 nm, which are assigned to the full-surface and interface modes, respectively. In the case of Ag NP, the experimentally measured spectrum shows much broader bands than the calculated ones, likely because the particle shape and contact with TiO_2 are not completely isotropic, the light incident angle is broad, and the light is not polarized. Because the same things should also hold for the Au NP and the separation of the two calculated peaks is smaller than that for the Ag NP, there is a possibility that the experimentally observed broad LSPR band of the Au NP consists of two broad, poorly separated LSPR modes. If so, each mode could be excited by irradiating with shorter- or longer-wavelength light.

With this in mind, Au nanosphere–TiO_2 samples were irradiated with light at 500–600, 600–700, or 500–700 nm (ca. 5 mW cm^{-2}, 30 min) to excite one or both the LSPR modes in the presence of SCN^- (in aqueous 1 M KSCN, pH was adjusted to ca. 4.0 using a phthalate buffer[27]). The light source was a Xe lamp (Luminar Ace LA-410UV, Hayashi Watch Works) equipped with a long-pass filter (≥500 nm, SCF-50S-50Y or ≥600 nm, SCF-50S-60R, Sigma Koki) and a short-pass filter (≤600 nm, GRF-530G or ≤700 nm, CLDM-50S, Sigma Koki). No spectral change was observed for a single Au nanosphere in the absence of SCN^- because of highly positive standard electrode potentials of Au (+1.83 and +1.53 V vs. NHE for $Au^{0/+}$ and $Au^{0/3+}$, respectively). In the presence of SCN^-, however, the potential shifted largely in the negative direction ($Au + 4SCN^- \rightarrow [Au(SCN)_4]^-$, +0.64 V vs. NHE),[28] and the scattering spectrum of a single Au nanosphere was changed by light irradiation (Figures 2a–2c). As the corresponding difference spectra clearly show, the scattering intensity decreases at around the irradiation wavelengths. When the sample was irradiated with 500–600-nm light, scattering intensity in this region decreased, and that in the longer wavelength region increased (Figure 2d). In the case of 600–700-nm light, the scattering intensity in this region decreased (Figure 2e). In addition, when we irradiated

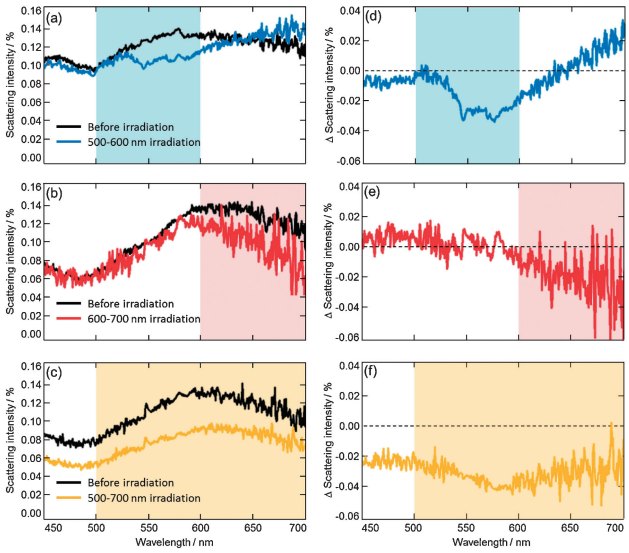

Figure 2. (a–c) Typical scattering spectra of a single Au NP (black) before and (colored) after light irradiation. (d–f) Difference spectra corresponding to panel a–c. Irradiation wavelength: (a, d) 500–600, (b, e) 600–700, and (c, f) 500–700 nm.

Table 1. Changes in the scattering intensity upon light irradiation

Irradiation wavelength/nm	Changes in the scattering intensity/%[a]	
	At 550 nm	At 650 nm
500–600	79.8 ± 5.1	105.5 ± 5.1
600–700	98.5 ± 3.9	79.7 ± 9.6
500–700	65.3 ± 17.4	64.2 ± 17.9

[a]Average ± standard deviation, $n = 5$.

the sample with 500–700-nm light, the scattering intensity was suppressed in the entire visible region (Figure 2f). The changes in the scattering intensity were reproducible, as summarized in Table 1. Such multiple spectral changes cannot occur if each single Au nanosphere exhibits only one LSPR mode. Therefore, we conclude that the broad LSPR band of a Au NP includes at least two LSPR modes, as predicted theoretically.

The spectral changes upon light irradiation should reflect certain morphological changes of the Au nanospheres, which must be caused by oxidative dissolution of Au ($Au + 4SCN^- \rightarrow [Au(SCN)_4]^-$) based on PICS. In the case of Ag NPs, it has been reported that the PICS-based oxidative dissolution of Ag proceeds preferentially at the sites where the plasmonic near field is strongly localized.[23] Regarding single Ag nanospheres on TiO_2, it has also been confirmed that the oxidative dissolution occurs at the entire particle surface and Ag–TiO_2 interfacial region, when the full-surface and interface modes, respectively, are excited.[13] Therefore, it is reasonable to expect that the site-selective oxidation also proceeds for Au nanospheres. We, therefore, calculated the scattering spectra for models based on this assumption (Figures 3a and 3b, inset). In both the models, it is assumed that 5% of Au is dissolved. The calculation results and the corresponding difference spectra are shown in Figure 3.

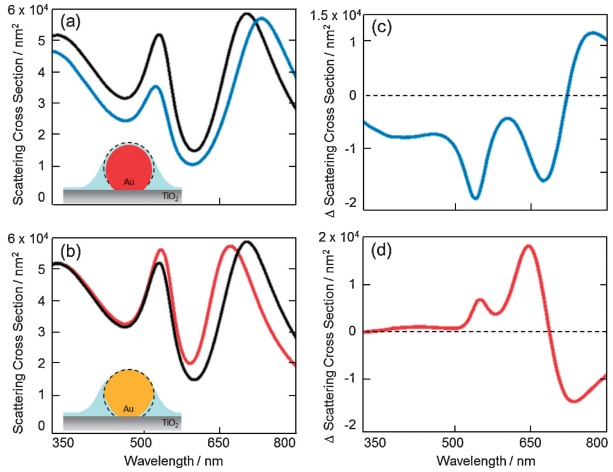

Figure 3. (a, b) Simulated scattering spectra (black) before and (colored) after morphological changes (insets). (c, d) Difference spectra corresponding to panel a and b.

When the oxidative dissolution of Au occurs at the entire surface and the particle becomes smaller by the full-surface mode excitation, the scattering intensity due to the full-surface mode decreases and the peak due to the interface mode slightly red shifts (Figure 3a). The corresponding difference spectrum (Figure 3c) is in good qualitative agreement with the experimental result (Figure 2d). On the other hand, in the case of selective dissolution at the interfacial region by the interface mode excitation, the peak based on the interface mode blue shifts (Figure 3b). In addition, the scattering intensity based on the full-surface mode slightly increases, and the difference spectrum (Figure 3d) shows an increase in the intensity around 500–650 nm. On the other hand, in the experimentally obtained difference spectrum (Figure 2e), no significant increase in the scattering intensity was observed even in the shorter-wavelength region, whereas the intensity decreased in the longer-wavelength region. This is because the separation between the full-surface and interface modes is not enough, as described above; therefore, the oxidative dissolution of Au proceeds not only in the interfacial region but also in other regions. Even so, we achieved the multiple spectral changes by light irradiation at different wavelengths, as shown in Figure 2. Irradiation at both wavelengths decreases the scattering intensity in the entre visible region, as shown in Figure 2f.

On the basis of the present wavelength-selective spectral changes, a commercially available and simple single Au nanosphere, which is smaller than the visible light wavelength, can serve as a two-wavelength optical memory device. Although thiocyanate is necessary for data writing, it can be easily removed by oxidation.[29] Therefore, the present system would allow the development of high-density, read-only optical memories with high stability. The present results can be simulated based on the assumption that the PICS-based oxidative dissolution of Au NPs proceeds preferentially at sites where the plasmonic near field is strongly localized, as is the case for Ag NPs.

In summary, photoinduced multiwavelength spectral changes were achieved for commercially available, single Au nanospheres (150-nm diameter) on TiO_2 based on the excitation of one or both the LSPR modes (full-surface and interface modes). Similar spectral changes can be simulated by assuming PICS-based oxidative dissolution of Au at the sites where the plasmonic near field is localized. Such multiple spectral changes of single Au nanospheres would allow application to stable multiple data storage nanodevices and nanooptical devices. Even smaller and higher-density devices might be developed by using smaller Au NPs.

This work was supported in part by JSPS Grant-in-Aid for Scientific Research on Priority Area "Coordination Programming" (Area No. 2107) No. 24108708 and Grant-in-Aid for Challenging Exploratory Research No. 25600002. I.T. thanks a JSPS Research Fellowship for Young Scientists.

References and Notes

† Present address: Department of Chemistry, School of Science and Technology, Kwansei Gakuin University, Hyogo 669-1337
1 K. L. Kelly, E. Coronado, L. L. Zhao, G. C. Schatz, *J. Phys. Chem. B* **2003**, *107*, 668.
2 K. A. Willets, R. P. Van Duyne, *Annu. Rev. Phys. Chem.* **2007**, *58*, 267.
3 M. E. Stewart, C. R. Anderton, L. B. Thompson, J. Maria, S. K. Gray, J. A. Rogers, R. G. Nuzzo, *Chem. Rev.* **2008**, *108*, 494.
4 S. Link, M. A. El-Sayed, *J. Phys. Chem. B* **1999**, *103*, 8410.
5 D. D. Evanoff, Jr., G. Chumanov, *J. Phys. Chem. B* **2004**, *108*, 13948.
6 R. Jin, Y. Cao, C. A. Mirkin, K. L. Kelly, G. C. Schatz, J. G. Zheng, *Science* **2001**, *294*, 1901.
7 K. L. Kelly, K. Yamashita, *J. Phys. Chem. B* **2006**, *110*, 7743.
8 G. Xu, M. Tazawa, P. Jin, S. Nakao, K. Yoshimura, *Appl. Phys. Lett.* **2003**, *82*, 3811.
9 Y. Ohko, T. Tatsuma, T. Fujii, K. Naoi, C. Niwa, Y. Kubota, A. Fujishima, *Nat. Mater.* **2003**, *2*, 29.
10 P. Zijlstra, J. W. M. Chon, M. Gu, *Nature* **2009**, *459*, 410.
11 K. Matsubara, T. Tatsuma, *Adv. Mater.* **2007**, *19*, 2802.
12 E. Kazuma, T. Tatsuma, *Chem. Commun.* **2012**, *48*, 1733.
13 I. Tanabe, T. Tatsuma, *Nano Lett.* **2012**, *12*, 5418.
14 Y. Tian, T. Tatsuma, *J. Am. Chem. Soc.* **2005**, *127*, 7632.
15 T. Tatsuma, *Bull. Chem. Soc. Jpn.* **2013**, *86*, 1.
16 Y. Tian, T. Tatsuma, *Chem. Commun.* **2004**, 1810.
17 T. Yamaguchi, E. Kazuma, N. Sakai, T. Tatsuma, *Chem. Lett.* **2012**, *41*, 1340.
18 Y. Takahashi, T. Tatsuma, *Appl. Phys. Lett.* **2011**, *99*, 182110.
19 Y. K. Lee, C. H. Jung, J. Park, H. Seo, G. A. Somorjai, J. Y. Park, *Nano Lett.* **2011**, *11*, 4251.
20 S. Mubeen, G. Hernandez-Sosa, D. Moses, J. Lee, M. Moskovits, *Nano Lett.* **2011**, *11*, 5548.
21 M. W. Knight, H. Sobhani, P. Nordlander, N. J. Halas, *Science* **2011**, *332*, 702.
22 E. Kowalska, R. Abe, B. Ohtani, *Chem. Commun.* **2009**, 241.
23 E. Kazuma, N. Sakai, T. Tatsuma, *Chem. Commun.* **2011**, *47*, 5777.
24 K. Naoi, Y. Ohko, T. Tatsuma, *Chem. Commun.* **2005**, 1288.
25 Y. Konishi, I. Tanabe, T. Tatsuma, *Chem. Commun.* **2013**, *49*, 606.
26 H. Nishihara, *Chem. Lett.* **2014**, *43*, 388.
27 Y. Konishi, I. Tanabe, T. Tatsuma, *Dalton Trans.* **2013**, *42*, 15937.
28 O. Barbosa-Filho, A. J. Monhemius, *Trans. Inst. Min. Metall., Sect. C* **1994**, *103*, C105.
29 I. R. Wilson, G. M. Harris, *J. Am. Chem. Soc.* **1960**, *82*, 4515.

